

MNHT2008-52118

EXPERIMENTAL STUDY OF OSCILLATING FLOW HEAT TRANSFER

Angie Fan, Doreen Fulmer and John Hartenstine

Advanced Cooling Technologies, Inc.
 1046 New Holland Avenue
 Lancaster, PA 17601, USA
 Phone: (717) 295-6061, Fax: (717) 295-6064
 angie.fan@1-act.com

ABSTRACT

This paper presents an experimental study of the heat transfer characteristics of mechanically driven oscillating flows inside small diameter channels and at various frequencies and stroke lengths. Two important parameters were studied: the effective thermal conductivity between the heat source and sink, and the heat transfer coefficients in the heating and cooling regions. The test data were compared to theoretical correlations in the literature to assess their validity in the operating range of interest. Kurzweg's correlation agreed reasonably well with the test data at low frequencies (1 Hz) and small amplitudes (7.6 cm). The highest effective thermal conductivity achieved during this study was more than 210,000 W/m-K. As a reference, pure copper and diamond materials have thermal conductivities around 400 W/m-K and 1,200 W/m-K, respectively. At low oscillating frequencies, the measured heat transfer coefficients in the heating region agreed reasonably well to Shin (1998)'s correlation. The correlation tends to under predict the heat transfer coefficient at higher frequencies. The experimental study investigated the effects of various frequencies and stroke length and demonstrated heat transfer coefficients in the heating region in excess of 34,000W/m²-K

Keywords: oscillating flow heat transfer, effective thermal conductivity, heat transfer coefficient

NOMENCLATURE

a area (m²)
 h heat transfer coefficient (W/m²-K)
 k_{eff} effective thermal conductivity (W/m-K)
 A sinusoidal oscillation amplitude (cm)
 A_c pipe cross-sectional area (m²)

A_f pipe inner surface area (m²)
 D tube inner diameter (cm)
 L tube length (cm)
 Nu Nusselt number
 Pr Prandtl number
 Q_{in} heat input (W)
 Q_{out} heat output (W)
 Re Reynolds number
 R thermal resistance (K/W)
 S oscillation tidal displacement (cm), S=2 x A
 T temperature (°C)
 T_{in/out} heat sink coolant inlet or outlet temperature (°C)
 Wo Womersley number, $W_o = \frac{D}{2} \sqrt{\frac{\omega}{\nu}}$

Greek Symbols

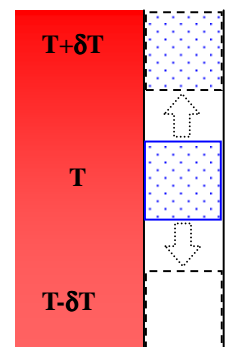
ω angular frequency of the oscillation,
 ω=2πf, where f is the frequency
 ν kinematic viscosity (m²/s)
 κ thermal diffusivity (m²/s)

Subscripts and superscripts

C cooling region
 H heating region

INTRODUCTION

Oscillating flows have the potential of being used for heat spreading applications for cooling of high power electronics and electrical equipment. Spreading heat with oscillating flow is



similar to spreading the flow with a pulsating heat pipe, [1], except the oscillating flow requires fluid movement by mechanical means instead of thermal input for the pulsating heat pipe. There are two modes of heat transfer with the oscillating flow: 1) single phase convective heat transfer from the oscillating fluid, and 2) evaporation and condensation heat transfer of the liquid and vapor. The heat spreading process is best visualized by looking at a small volume of fluid in a single tube as shown in the sketch at right. The fluid has no net motion but simply oscillates back and forth. The slug of fluid comes to equilibrium at temperature T . If it oscillates up, it will be next to a wall which is at $T+\delta T$ so the slug will absorb heat from the wall and raise its temperature (a portion of the fluid undergoes phase change). When it moves down, it will be at a higher temperature than the adjacent wall and give up heat to the wall. While its oscillation amplitude is small, each slug provides a net transport of heat from top to bottom. Other slugs above and below it will repeat this process, resulting in macroscopic heat transport from the load to the sink. This oscillation transfers (or spreads) heat with extremely high efficiency, particularly at high oscillating frequencies.

A number of other researchers have investigated oscillating flow heat transfer, such as Kurzweg [2-4]. Kurzweg [2] evaluated the heat transfer between two reservoirs that were held at different temperatures and connected using glass capillary tubes. The fluid inside the tubes was oscillated using a vibrator between 2 and 8 Hz. It was found that the effective thermal diffusivity is proportional to the square of the tidal displacement also known as stroke length and the square root of the oscillating frequency. The work presented herein describes an experimental study to measure and calculate the effective thermal conductivity and heat transfer coefficients for various amplitudes, frequencies and distance between the heat source and sink to potential heat spreader applications for cooling power electronics.

EXPERIMENTAL SETUP

An experimental test article was designed and fabricated to study the heat transfer characteristics of mechanically driven oscillating flows inside small diameter channels. A schematic of the apparatus is shown in Fig. 1 and 2. The apparatus consists of a copper flow tube, a heater block to provide heat input to the test section using an electric cartridge heater, heat sink(s) to remove heat from the test section and a mechanically driven fluid oscillator. The total length of the oscillating flow tube was 0.81m. The flow tube inside diameter was 2.4mm, with a wall thickness of 0.41mm. A copper heater block was brazed onto the test section. The contact area between the heater block and the flow tube was 0.63cm^2 . Two type K thermocouples (T_{H1} and T_{H2}) were inserted into the heater block body. The thermal power delivered to the oscillating flow loop can be measured knowing the temperature gradient between the two thermocouples and the physical thermal conductivity properties of the heater block.

$$Q_{in} = (T_{H1} - T_{H2}) \cdot R_{k1} \quad (1)$$

Copper heat sinks were attached to the flow tube. The contact area was 5.07cm^2 . Depending on the test configuration, one or two liquid-cooled heat sinks were soldered onto the test section. The inlet and outlet temperatures of the coolant flows were measured to calculate the Q_{out} .

$$Q_{out} = \dot{m} \cdot c_p \cdot (T_{out} - T_{in}) \quad (2)$$

A series of tests were performed to evaluate the impact on the effective thermal conductivity by varying the number of heat sinks within the oscillating loop and their relative location from the evaporator block. These configurations and their respective geometries are listed in table 1 and Figure 2. The actuator and drive assembly generate fluid oscillations at predefined oscillating strokes and frequencies

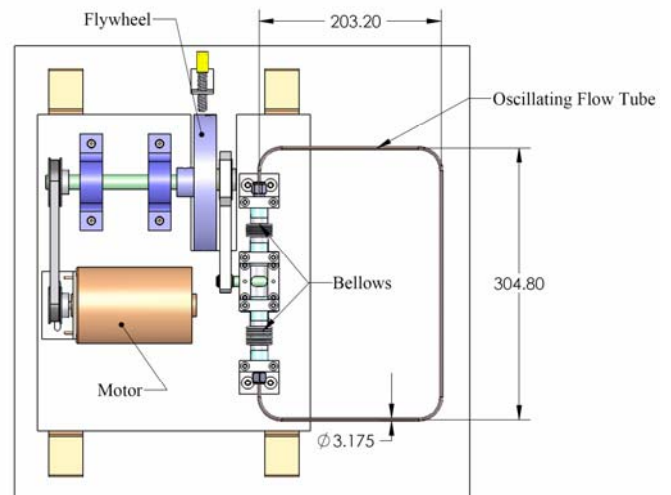


Figure 1 Schematic of experimental apparatus (length in mm)

Table 1 Heater and heat sink configurations

Configuration	Number Heat Sinks	L_{HC} (mm)
A	1	152
B	1/2	305
C	1	610

The copper flow tube was instrumented with Type T thermocouples at 50 mm increments between the evaporator and condenser. The schematic shown in Figure 3 details the thermocouple locations along the oscillating flow loop. A computerized data acquisition system was used to gather and record the temperatures during testing.

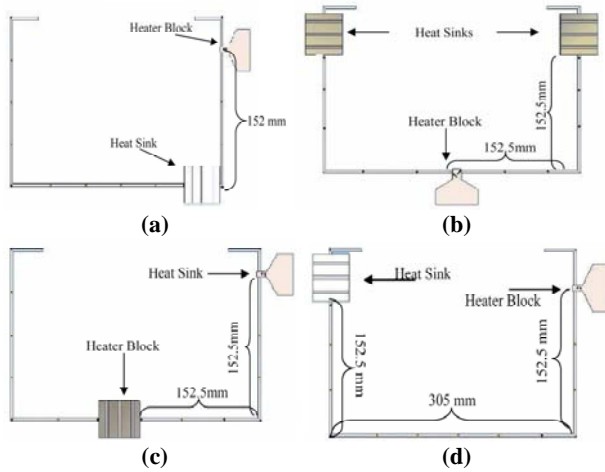


Figure 2 Oscillating flow test configurations: (a) Configuration A - 152 mm Length between Heater Block and Heat Sink. (b) Configuration B – 2 Heat Sink 305 mm between Heater Block and Heat Sink. (c) Configuration B – 1 Heat Sink 305 mm between Heater Block and Heat Sink. (d) Configuration C – 610 mm between Heater Block and Heat Sink.

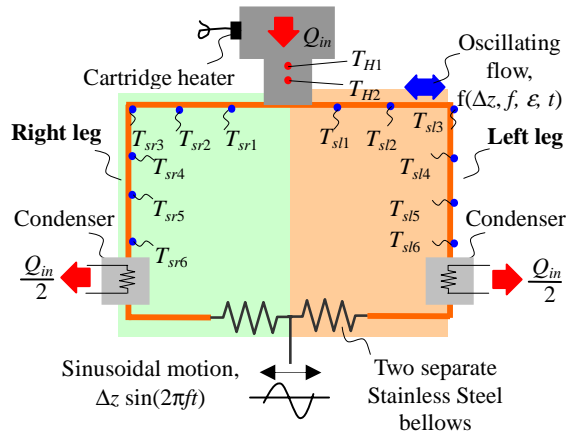


Figure 3 Oscillating flow schematic detailing thermocouple locations and test set up. This configuration is for configuration (b) in Figure 1.

Comparing the thermal power applied to the flow loop, Q_{in} , with the condenser calorimetry, Q_{out} , confirmed that the heat loss from the test apparatus to the ambient was less than 10% of the heat input.

The fluid oscillator consisted of a motor, a flywheel, a slide mechanism and two metallic bellows. A fill tube was attached to the end cap of one of the bellows to allow evacuating and charging of the system with the working fluid, in this case water was used. The fill tube was also used to pressurize the internal volume of the system to 3.1Bar. This was designed to avoid premature boiling incipience in the system. The saturation temperature of water at 3.1Bar is 135°C.

The magnitude of the stroke length was set by adjusting the displacement of the bellows. Table 2 lists the stroke lengths used in the experiments and the corresponding sinusoidal amplitudes.

Table 2 Stroke length settings

Bellows Displacement (mm)	Stroke Length (mm)	Amplitude (mm)
0.75	76	38
1.3	152	76

The frequency was measured and controlled by a photo-eye and a frequency counter. Three frequencies, 1Hz, 2Hz and 10Hz, were used for each of the established stroke lengths (Table 2).

The frequency and amplitude of the oscillating water and the distance between the heat input and output regions were varied in the experiments to investigate their effects on the following three performance parameters: effective thermal conductivity of the flow loop, and both the heating and cooling convective heat transfer coefficients. The effective thermal conductivity is determined as follows:

$$k_{eff} = \frac{Q_{in} \cdot \Delta x}{A_c \cdot \Delta T} \quad (3)$$

where $\Delta T = T_H - T_C$ is the temperature difference and Δx is the distance between the heat source and the heat sink, respectively. The convective heat transfer coefficient for the heating region was determined as follows:

$$h = \frac{Q_{in}}{A_{fH} (T_{H5} - T_{f0})} \quad (4)$$

The fluid temperature, T_{f0} , was the average of the readings of the two thermocouples nearest to the heat source, and T_{H5} was the inner wall temperature right below the heat source. The heat transfer coefficient for the cooling region as determined as follows:

$$h = \frac{Q_{in}}{A_{fC} (T_C - T_{watercooling})} \quad (5)$$

The fluid temperature, T_C , was the reading of the thermocouple nearest to the heat sink, and $T_{watercooling}$ was the average of the readings of the two thermocouples at the inlet and outlet of the coolant flow.

Figure 4 shows the thermal circuit model at the electric heater block from the measured temperatures (T_{H1} , and T_{H2}) to the fluid temperature, T_{f0} . As shown in Fig. 4, using the dimensions and thermo-physical properties of the copper heater block, the actual conduction heat Q_{in} is calculated from the measured heater temperatures of T_{H1} and T_{H2} .

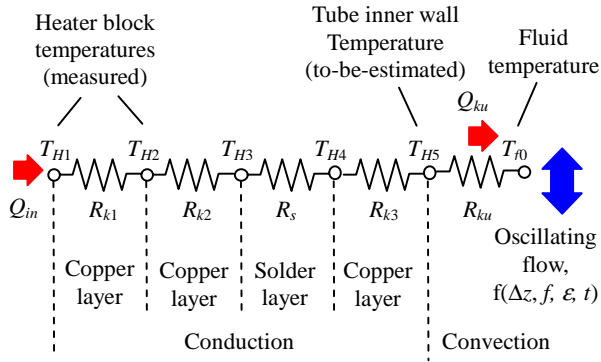


Figure 4 Thermal circuit model at the electric heater block from measured temperatures to the fluid temperature.

The additional temperatures T_{H3} , T_{H4} , and T_{H5} along the heat transfer path toward the tube are also estimated using the distances between temperatures assuming one-dimensional conduction. The tube inner wall temperature is expressed as the following equation.

$$T_{H5} = T_{H2} - Q_{in}(R_{k2} + R_s + R_{k3} + R_{ku})$$

$$Q_{in} = (T_{H1} - T_{H2})R_{k1}$$

(6)

where

$$R_{ki} = \frac{L_i}{k_{cu}(T_{H2})A_i}, \text{ where } i = 1, 2, 3,$$

$$R_s = \frac{L_s}{k_s A_s}, \text{ and } R_{ku} = \frac{1}{h_f A_f}.$$

Testing was performed on the oscillating flow loop for each configuration. The amplitude and frequency were established. The assembly was insulated to reduce thermal losses to ambient. The heaters within the heater block were energized in increments of approximately 10W and maintained until steady state was reached. The water cooling flow rate was 120ml/min.

EXPERIMENTAL RESULTS

Effective Thermal Conductivity

The effective thermal conductivity k_{eff} as determined by Equation (3) includes the effects of the copper wall and the oscillating flow. The various conditions in the experiments yielded k_{eff} values ranging from 8.6×10^3 W/m-K to 2×10^5 W/m-K. The highest k_{eff} corresponds to an effective thermal conductivity that is more than 500 times the thermal conductivity of copper.

It was observed that within certain ranges of frequency and amplitude, the effective thermal conductivity is proportional to the amplitude and the square root of the frequency, as pointed out by Kurzweg [2]. This behavior is recorded in Fig. (5-9). These figures detail the heat input, as measured through conduction calorimetry, versus the temperature difference between the heating and cooling regions at various frequency,

amplitudes and stroke lengths. Since $\frac{\Delta x}{A_c}$ (referring to Eq. 3)

is a constant in each figure, the slopes of the lines in these figures represent the relative values of the effective thermal conductivity.

Figure 5 compares the single branch configuration to the double branch configuration (referred to Table 1 as Configuration B). It can be seen that there is no significant difference between the thermal conductivity measurements for the two configurations.

Close examinations of Fig. (5-9) indicate that, above certain oscillation amplitudes and frequencies, the enhancement of the effective thermal conductivity by the further increases in amplitude and frequency is limited. This may be due to the “drag” effect from the heat capacity and thermal conductivity of the copper wall and the heat transfer ability in the heating and cooling regions. The effective thermal conductivities became smaller at 10Hz compared to 2Hz for the largest amplitude setting $A=15.24$ cm. It was also observed that increasing the heat source-to-sink distance can improve the effective thermal conductivity. These results may be due to the two-phase phenomenon in the system.

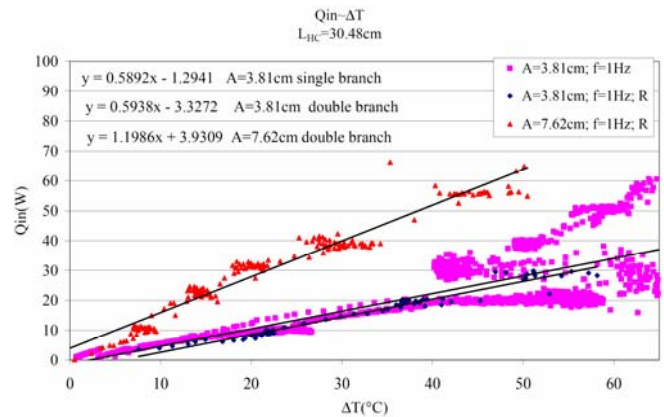


Figure 5 Heat input vs. ΔT at $f=1$ Hz, $L_{HC}=30.48$ cm.

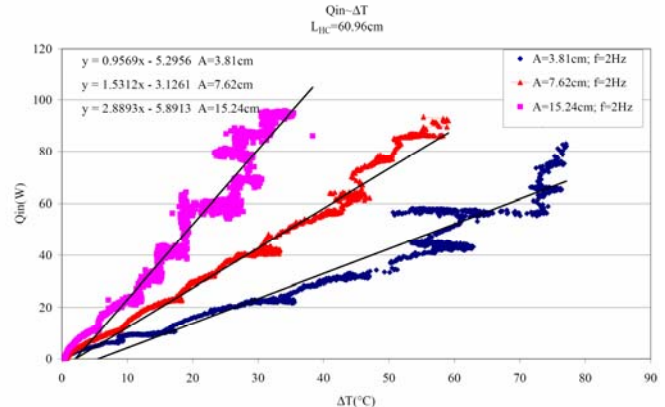


Figure 6 Heat input vs. ΔT at $f=2$ Hz, $L_{HC}=60.96$ cm.

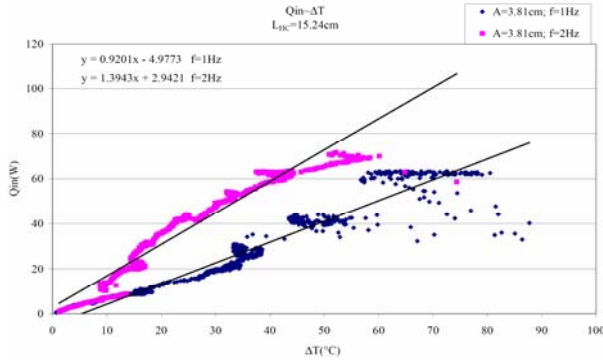


Figure 7 Heat input vs. ΔT at $A=3.81$ cm, $L_{HC}=15.24$ cm.

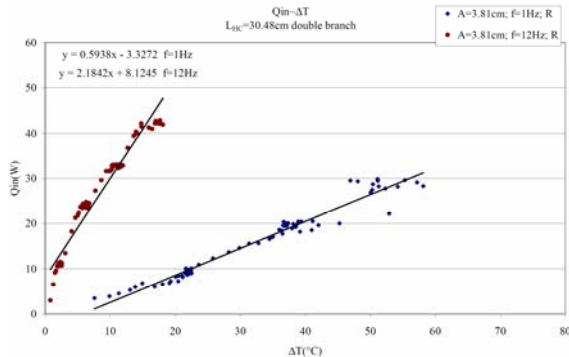


Figure 8 Heat input vs. ΔT at $A=3.81$ cm, $L_{HC}=30.48$ cm.

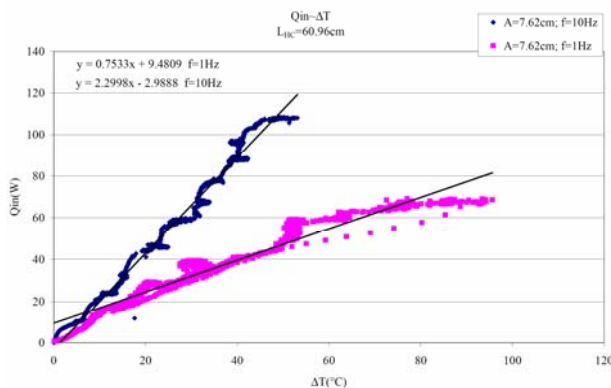


Figure 9 Heat input vs. ΔT at $A=7.62$ cm, $L_{HC}=60.96$ cm.

Effective heat transfer coefficients

Table 3 summarizes the different frequencies, amplitudes, test section diameters, heating section length, cooling section length, and heat source-to-sink distance that were investigated.

Table 3 Summary of all testing configurations

oscillation frequencies	1Hz, 2Hz, 10Hz, 12Hz
oscillation amplitudes	3.81cm, 7.62cm, 15.24cm
L_{HC}	15.24cm, 30.48cm, 60.96cm
tube diameter	0.3175cm(OD) x 0.2362cm (ID)
L_H	0.635cm
L_C	5.08cm

Figures (10-15) show the relationship between the heat input and the temperature difference in the heating region (or in the cooling region) under different configurations, referring to Eq. (6-7). The surface area of the fluid at the heating region A_{FH} is $4.7 \times 10^{-5} \text{ m}^2$, and that at the cooling region A_{FC} is $37.6 \times 10^{-5} \text{ m}^2$. The slopes of these lines $\frac{Q_{in}}{\Delta T} = \frac{h}{A_f}$ reveal the relative

values of the effective heat transfer coefficient. Note that the heat transfer coefficients at the heating region were calculated within the oscillating flow, while the heat transfer coefficients at the cooling region were between the oscillating flow and the cooling water (in between were copper walls). Therefore, the values of the cooling region heat transfer coefficients are smaller than that within the oscillation flow area but the trends against different factors are analogous. The heat source-to-sink distance L_{HC} is 15.24cm in Fig. 10, 30.48cm in Fig. (11-12), and 60.96cm in Fig. (13-15).

Consistent trends were observed in most heat transfer coefficient measurements. These trends include:

- Higher oscillation frequencies yield higher heat transfer coefficients
- Larger amplitudes yield higher heat transfer coefficients.
- The relationship between the amplitude and length affects heat transfer
- The heat source-to-sink distance L_{HC} has little impact on the heat transfer coefficient

Oscillation Frequency Affects

In Fig. (16-17) T_{i0} is the bulk fluid temperature and T_{H5} is the wall-fluid interface temperature in the heating region. By increasing the frequency from 2Hz to 10Hz and keeping all the other parameters unchanged, both temperatures, especially the wall temperature T_{H5} decreased significantly.

The plug-like velocity profiles developed at high frequencies improve the convective heat transfer. A high frequency results in a larger Womersley number Wo . Womersley number is a dimensionless expression of the pulsatile flow frequency in relation to viscous effects. When Wo is 1 or less (i.e. the frequency is sufficiently low), a parabolic velocity profile has time to develop during each cycle. When Wo is 10 or more, the frequency is sufficiently large that the velocity profile is relatively flat or plug-like, as shown in Fig. 19(a). In our experiments, the Womersley number varied from 5 to 50, which is from the transient to the plug-like velocity regime. The Prandtl number of the liquid water in our experiments was between 1 and 5 (depending on the temperature). This indicates a similarity between the heat diffusion and the viscous dissipation. In other words, the temperature profile closely tracks the velocity profile. The plug flow pattern corresponds to a thinner thermal boundary layer which helps heat transfer from the tube inner wall to the bulk flow (or vice versa in the cooling region). The plug flow

pattern, with a more uniform radial temperature profile, carries more internal energy than the parabolic flow pattern during each stroke. This helps axial heat transfer. The plug flow velocity profile can reach an ultimate limit when the boundary layer is extremely thin.

Amplitudes Effects

Figure 16 and 18 show the tube inner wall and fluid temperatures in the heating region at two different amplitudes, 7.62cm and 15.24cm. Both temperatures decreased as amplitude increased, which indicate better heat transfer. The wall temperature decreased more significantly.

At the edge of the heating or cooling sections, a larger amplitude helps transport high internal energy mass flow further along the axial direction where the mass flow has lower internal energy, as is shown in Fig. 19(b).

Amplitude and the Length Relationship Effects

The ratio between the amplitude and the length of the heating or cooling region affects the heat transfer within the heating or cooling region. The principle of the oscillating flow heat transfer is exchanging heat between higher energy portions of the flow with the adjacent, low energy portions of the flow, which is as analogous to the “bucket-brigade” action. The cooler the area that the higher energy portion of the flow can reach, the more heat can be transferred. In a hypothetical case of $A/L \ll 1$, the length of the heating region is so large that only the flow portion close to the edge of the heating region can directly contact the cooler fluid outside of the heating region. Consequently, the heat exchange between the cooler fluid outside of the heating region and the hotter fluid in the center of the heating region is ineffective. On the contrast, if $A/L \gg 1$, getting the heat from the hotter fluid in the heating region is no longer a problem, since the large amplitude can move all the hotter fluid to outside of the heating region to have direct, effective heat exchange with the cooler fluid there. This explains why in our case, the heat transfer coefficients in the heating region were much higher than in the cooling region at the following A/L ratios: $A/L_H = 6, 18, 24$, and $A/L_C = 0.75, 1.5, 3$. It also explains why the heat transfer coefficients in the cooling region showed the same trends as in the heating region at a large amplitude of 6”, and why for smaller amplitudes of 1.5” and 3”, the changing in frequencies is less effective (the heat is not effectively received by the cooling region).

Heat Source-to-Sink Distance Affects

The distance between the heating and cooling regions only affects the heat transfer length, so that for longer distance it will take longer time for the flow to reach steady state. Once the steady state is reached, the distance won’t have any impact on the local heat transfer in the heating or cooling region.

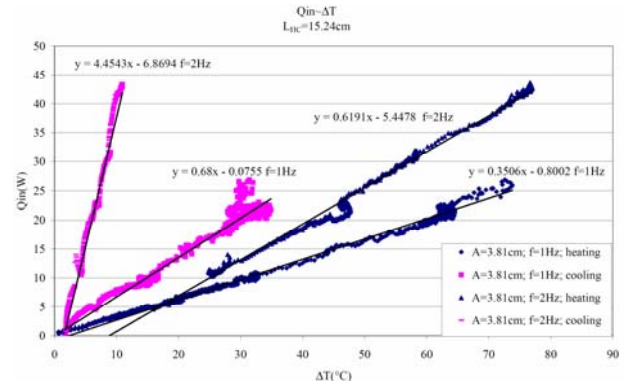


Figure 10 Heat input vs. ΔT at $A=3.81\text{cm}$, $L_{HC}=15.24\text{cm}$.

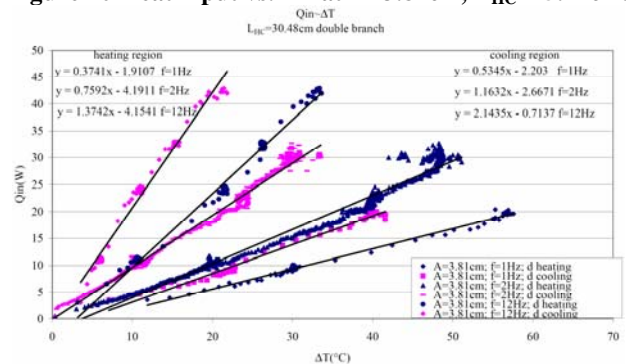


Figure 11 Heat input vs. ΔT at $A=3.81\text{cm}$, $L_{HC}=30.48\text{cm}$.

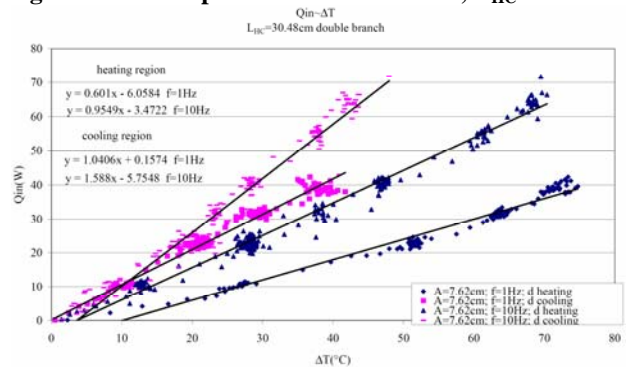


Figure 12 Heat input vs. ΔT at $A=7.62\text{cm}$, $L_{HC}=30.48\text{cm}$.

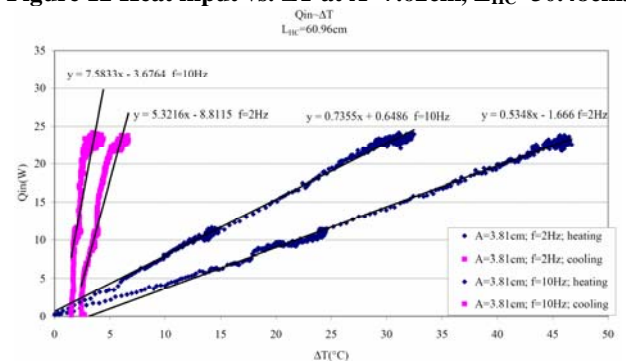


Figure 13 Heat input vs. ΔT at $A=3.81\text{cm}$, $L_{HC}=60.96\text{cm}$.

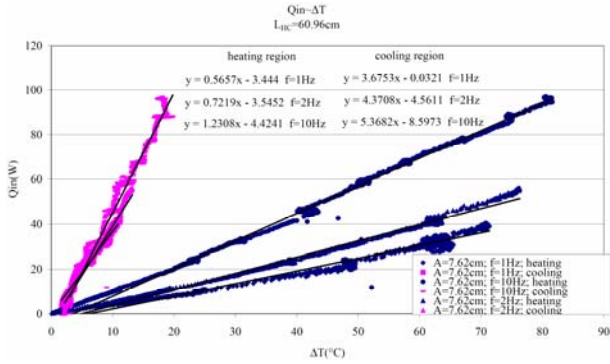


Figure 14 Heat input vs. ΔT at $A=7.62\text{cm}$, $L_{HC}=60.96\text{cm}$

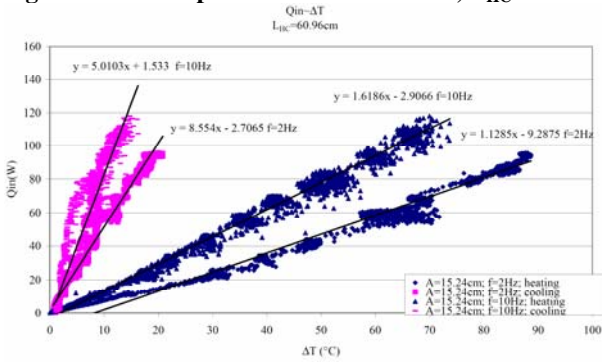


Figure 15 Heat input vs. ΔT at $A=15.24\text{cm}$, $L_{HC}=60.96\text{cm}$

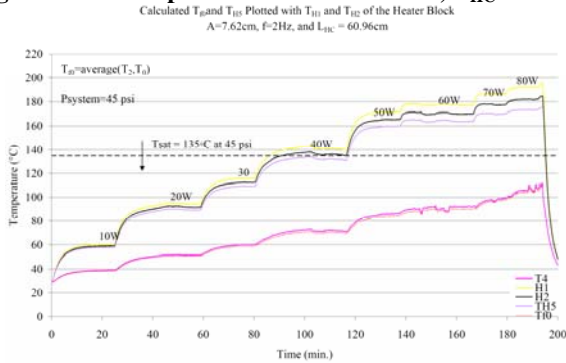


Figure 16 T_{H5} and T_0 under different heat inputs at $A=7.62\text{cm}$, $f=2\text{Hz}$, $L_{HC}=60.96\text{cm}$

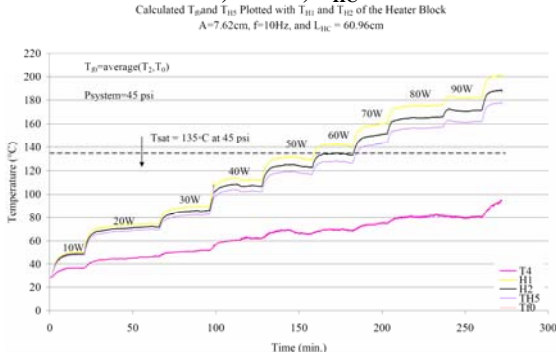


Figure 17 T_{H5} and T_0 under different heat inputs at $A=7.62\text{cm}$, $f=10\text{Hz}$, $L_{HC}=60.96\text{cm}$

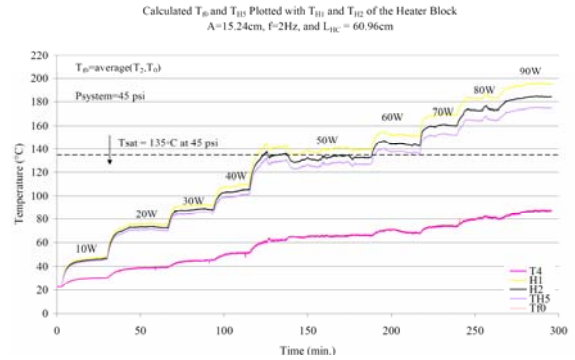


Figure 18 T_{H5} and T_0 under different heat inputs at $A=15.24\text{cm}$, $f=2\text{Hz}$, $L_{HC}=60.96\text{cm}$

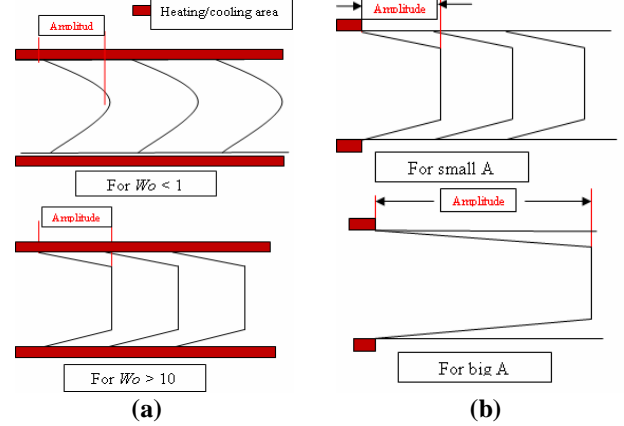


Figure 19 (a) Velocity profiles of the oscillation flow under low frequency ($Wo < 1$) and high frequency ($Wo > 10$). (b) Velocity profiles of the oscillation flow with small amplitude and big amplitude

Comparisons with previous Correlations

This section compares our experimental results with Nishio and Shin's correlations.

Nishio et al. [5] developed the following correlation to calculate the effective thermal conductivity of an oscillating flow as follows:

$$k_{eff} = \begin{cases} \rho C_p \left(\frac{0.707}{1 + \frac{1}{Pr}} \left(1 + \frac{1}{\sqrt{Pr}} \right) \left(\frac{S^2}{D/2} \right) \sqrt{\omega \kappa} \right), & Wo > 1 \\ \rho C_p \cdot \frac{1}{96} \left(1 - \frac{13Pr^2 + 3}{2880} \cdot \left(\frac{D}{2} \sqrt{\frac{\omega}{\nu}} \right)^4 \right) \cdot \left(\frac{DS}{2} \right)^2 \left(\frac{\omega^2}{\kappa} \right), & Wo \leq 1 \end{cases} \quad (7)$$

Generally, Nishio's correlation tends to under-predict the thermal conductivity at small amplitude, as is shown in Fig. 20. At large amplitude, the increase of experimental thermal conductivity slowed down or stopped due to various limitations such as heat capacity and thermal conductivity of the copper wall. On the other hand, Nishio's curve keeps increasing

without accounting for the effect of wall's heat capacity and thermal conductivity.

Shin *et al.*[6] numerically investigated the heat transfer effects at heating and cooling regions in oscillation flow tubes and modified formula for heat transfer coefficient based on Hausen's equation for the heating region, as follows:

$$Nu_D = 3.3Wo^{0.2} + \frac{0.025(A/L_h)Wo^2 Pr}{1 + 0.016[(A/L_h)Wo^2 Pr]^{2/3}} \quad (8)$$

and for the cooling region:

$$Nu_D = 3.3Wo^{0.2} + \frac{0.041(A/L_c)Wo^2 Pr}{1 + 0.016[(A/L_c)Wo^2 Pr]^{2/3}} \quad (9)$$

Both equations are assumed to have extremely thin wall system; therefore the heat transfer coefficients are independent of the thermal characteristics of the tube wall.

Compare with the experimental effective heat transfer coefficients at the heating region, Shin's correlation trends to under-predict the results, as is shown in Fig. 21.

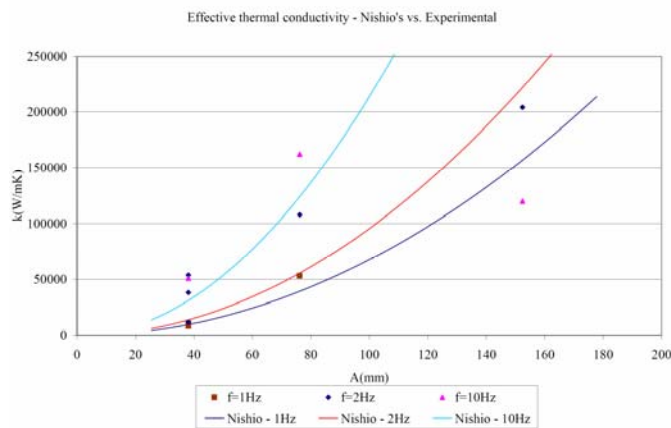


Figure 20 Effective thermal conductivity – Nishio's vs experimental data.



Figure 21 Effective heat transfer coefficient at heating region – Shin's vs experimental data.

CONCLUSIONS

The followings conclusions are drawn from the oscillating flow tests and analysis performed:

1. The effective thermal conductivity of the oscillating flow pipe is observed to be proportional to the oscillation amplitude and the square root of the oscillation frequency within certain range.
2. Above certain frequency and amplitude range, further enhancement of the effective thermal conductivity is limited, which may be due to the "drag" effect from the heat capacity and thermal conductivity of the copper wall and the heat transfer ability in the heating and cooling regions.
3. The effective heat transfer coefficient is related with oscillation amplitude and frequency, length of the heating or cooling regions.
4. Previous theoretical correlations based on models that neglect the thermal characteristics of the wall system tend to under predict both the thermal conductivity and heat transfer coefficient.

ACKNOWLEDGEMENT

This work was sponsored by the U.S. Navy under Contract No. N65540-06-C-0012. Mr. Mark Zerby, NSWC was the technical monitor on this contract. The authors would also like to acknowledge the fabrication and test support provided by Mr. Jesse Campbell of Advanced Cooling Technologies, Inc.

REFERENCES

- [1] Akachi, H., 1990, "Structures of a Heat Pipe", U.S. Patent # 4,921,041.
- [2] Kurzweg, U.H., 1985, "Enhanced Heat Conduction in Fluids Subjected to Sinusoidal Oscillations", *Journal of Heat Transfer*, Volume 107, pp 459-462
- [3] Kurzweg, U. H., and Zhao L., 1984, "Heat transfer by high-frequency oscillations: A new hydrodynamic technique for achieving large effective thermal conductivities," *Phys. Fluids* 27 (11), pp. 2624-2627.
- [4] Kurzweg, U. H., 1986, "Temporal and spatial distribution of heat flux in oscillating flow subjected to an axial temperature gradient," *Int. J. Heat Mass Transfer.*, vol. 29, No. 12, pp. 1969-1977.
- [5] Nishio, S., Shi, X., and Zhang, W., 1995, "Oscillation-induced heat transport: heat transport characteristics along liquid-columns of oscillation-controlled heat transport tubes," *Int. J. Heat Mass Transfer.*, vol. 38, No. 13, pp. 2457-2470.
- [6] Shin, H., and Nishio, S., 1998, "Oscillation-controlled heat transport tube (heat transfer coefficient in tubes in heating and cooling regions)," *Heat Transfer-Japanese Research*, 27(6).